

MAGNETIC FILTRATION TRENDS OF MULTI-FUNCTIONAL MAGNETIC NANOPARTICLES WITH RESPECT TO ITS SIZE AND ENVIRONMENTS DURING SEVERE ACCIDENT

D.H. Kam, and Y.H. Jeong*

Korea Advanced Institute of Science and Technology

Department of Nuclear and Quantum Engineering, Korea Advanced Institute of Science and
Technology, 291, Daehak-ro, Yuseong-gu, Daejeon, 305-701, Republic of Korea

idcandy@kaist.ac.kr; jeongyh@kaist.ac.kr

ABSTRACT

In this study, application of magnetic nanoparticles, consists of magnetite as a core material and surrounding porous structures with functional groups attached on the surfaces, is considered during activation of the severe accident mitigation strategies. The system can enhance a thermal margin (Critical Heat Flux) and decontaminate the coolant as well during the operation. Also, with a magnetic filtration system, environmental release could be prevented by localizing the target radionuclides. Success of the whole system is strongly affected by the magnetic filtering system that roles a boundary component before the release. By changing sizes of magnetite and porous structures, filtering efficiency is affected, and on this basis, size effects of these parameters has been mainly considered in this study. According to the calculation results, the collection efficiency increases with a magnetic particle size and decreases with a coating thickness. It decreases with temperature, but the temperature effect is marginal compared with other parametric effects.

KEYWORDS

Severe accident, Magnetic nanoparticle, CHF, Decontamination

1. INTRODUCTION

Radioactive nuclides are ejected throughout a containment during a severe accident progression, and mitigation strategies like IVR-ERVC (In-Vessel Retention of molten corium through External Reactor Vessel Cooling) and core catcher are activated to ensure the integrity of the containment. During the operation, since decay heat from the molten corium is removed by natural circulation of a coolant and boiling process, overall heat transfer performance including thermal margin (critical heat flux, CHF) becomes crucial to guarantee the success of the system. Radioactive nuclides such as Cs and I are dissolved inside the coolant, and environmental impacts could be enormous if released through the containment. In this regard, a system consists of magnetic nanoparticles and magnetic collector is suggested in this study; the CHF enhancement, decontamination and localization of the radioactive nuclides can be achieved through the system.

Nanofluid is composed of suspended nano-sized particles and bulk fluid, and usually applied to industries by its enlarged surface area. For systems with high heat flux condition, nanofluids can enhance the thermal margin by deposition during boiling process. Porous structures, that enhance fluid supply near the CHF

* Footnote, if necessary, in Times New Roman font and font size 10

point, are formed by the deposition. In this regard, preceding studies have been widely performed focusing on the CHF enhancement with the nanofluids [1-5]. Under nucleate boiling heat transfer conditions, the nanofluid system tended to show notably enhanced results even though there still seems some slight increment or sometimes even degraded results. However, when application of the nanofluid to nuclear power plants is considered, there are some limitations like dispersion state and collection after usages. In Lee et al. [6]'s study, effects of dispersion state on the CHF results have been addressed, and pressure, dilution and storage time effects have been also considered to reflect real applications during accidental conditions. Through the study, necessity of dispersion on the CHF enhancement and steady increase with pressure were shown. Also, dilution effect based on the initial concentration has been assessed to minimize storage volume inside the nuclear power plant, and continuous increase of particle size with storage time by agglomeration has been measured, which showed negligible enhancement beyond certain periods of the storage time. To solve the collection problem, Lee et al. [6-8] used magnetite nanoparticles, that show enormous magnetic force when an external magnetic field is applied, in pool and flow boiling systems. Lee et al. [7] used the magnetic property of the particles to further enhance the CHF margin, which suggests potential way to collect the nanoparticles, and Lee et al. [8] assessed flow regime effects on the CHF enhancement when surface wettability condition was improved by the nanoparticle deposition. The enhancement was noticeable for nucleate boiling regimes, and it tended to show decreased enhancement as the regime approached to annular flow regimes. With the magnetic properties, nanoparticles can be gathered and collected by flowing them through the collector part where ferrite cores are located inside and an external magnetic field is applied. The magnetic nanoparticles can be collected at the surface of the ferrite cores where field gradient is made. The phenomenon is called 'magnetic filtration.'

Several researches including calculations and experiments have been performed on the magnetic filtration considering geometrical and environmental conditions. Generally, force balance equations, where a magnetic attraction force term is included, are used to calculate the amount and shape of accumulations around the ferrite cores when an external magnetic field is applied. Watson [9] derived net forces, in radial and tangential directions, on magnetic particles, and Uchiyama et al. [10] considered wire-shaped ferromagnetic ferrite cores in their calculations based on the Watson's approach. Similarly, Oberteuffer [11] calculated the magnetic filtration effect with ferromagnetic filaments, but with CuO powders. Based on the results, relative size effect between the particle and the filament has been summarized. Several kinds of particles, including the magnetite, and steel wires as ferrite cores were considered by Takayasu et al. [12] for the magnetic filtration. They have considered field strength effect along with the temperature conditions in their calculations. A gravitational force term has been included in Ying et al. [13]'s study, and relative directions between flow, gravitational and magnetic forces has been considered to simulate the accumulation area around surfaces of the ferrite cores. Later, Moeser et al. [14] further included a diffusion force term, made by a concentration difference between the accumulated regions and a bulk fluid, into the Ying et al.'s equations. In their approach, they firstly calculated purely drag-limited and purely diffusion-limited net forces where diffusion force term and drag force term are neglected, respectively. Accumulation area around a steel wire, that roles as a ferrite core, were calculated from overlapping area between the two forces. Especially, they have included coating thickness term in their derivation to account for coated magnetic particles. Calculated results have been compared with experimental data acquired in their other papers. In Friedlaender et al. [15]'s study, collection of the magnetic particles has been captured with a camera where a single array and multiple arrays of the wires were prepared. Relationship between the flow speed and accumulation radius has been summarized and plotted.

When target nuclides are concerned, there are specific functional groups that show great combination with target nuclides. Proper selection of the functional groups guarantees outstanding attachment with high selectivity against other competing ions compared with conventional methods, and the efficiency is strongly affected by pH condition, kinds of competing ions dissolved, temperature, etc. Granados et al. [16] and Feng et al. [17] performed experiments on the capturing efficiency considering the aforementioned environments

but temperature condition. They mainly focused on the Cs ion capture when other competing ions like Na^+ was dissolved inside various pH conditions.

Based upon the aforementioned characteristics and technologies, a system with multi-functional magnetic nanoparticles and collector part has been suggested to enhance heat transfer performance of the severe accident mitigation strategies and to decontaminate target radioactive nuclides, especially Cs ion, inside the coolant during the operation of the strategies. To assess the applicability of the system, the collector part has been mainly focused, and especially, effects of particle size with temperature conditions have been considered in this study.

2. OVERALL SYSTEM AND POTENTIAL APPLICATIONS

Based upon the realized technologies from other areas, a combined system has been proposed to the nuclear power plants in this section. Firstly, a magnetic nanofluid is considered as a coolant for the severe accident mitigation strategies to fulfill the several objectives at the same time: Enhancement of the heat transfer performance, decontamination & localization of the target nuclide and waste minimization. For the purpose, the particle consists of a magnetite at the center, porous silica coating around the core and specific functional groups (or functional arms) attached on the silica (Fig. 1). By applying an external magnetic field, the magnetite is magnetized, which leads to the collection. The porous structures around it induces an enlarged surface area, which, in turn, increases number density of the functional groups. The number density can be maximized by the nano-sized particles and the porous structures.

Through the aforementioned characteristics and properties, the system can be applied to the severe accident mitigation strategies. By injecting the multi-functional magnetic nanoparticles inside the coolant, the CHF margin can be improved, and the target radioactive nuclide, especially Cs ion, can be steadily captured through bonding between the functional arms and the nuclide. After the usage, purified coolant can be ejected by flowing the contaminated nanofluid through the collector part.

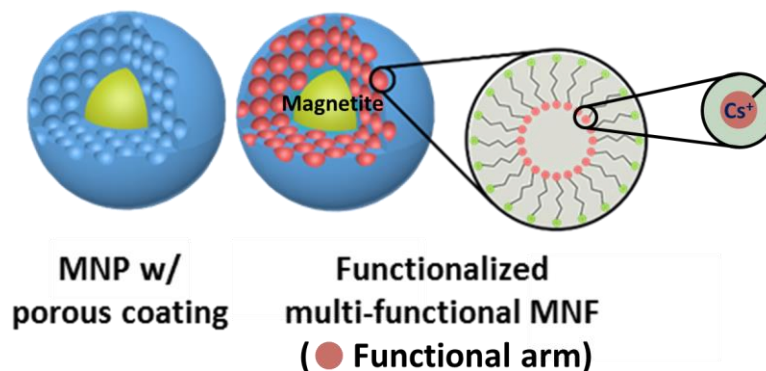


Figure 1. Multi-functional magnetic nanoparticle (Magnetite-porous silica coating-functional groups).

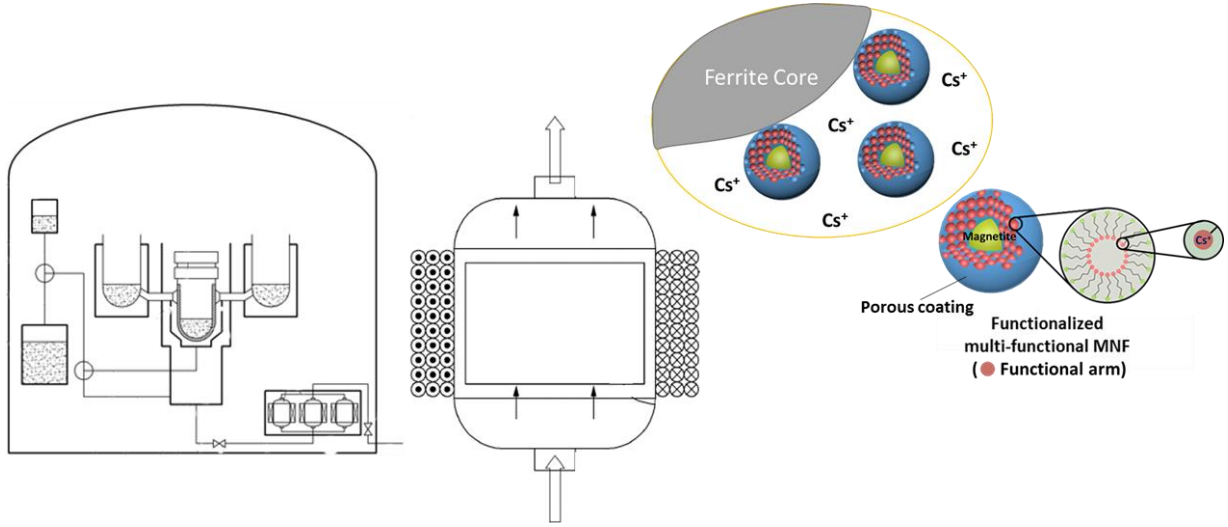


Figure 2. Multi-functional magnetic nanoparticle application to the IVR-ERVC strategy.

3. BASIC EQUATIONS FOR MAGNETIC PARTICLE COLLECTION AROUND A WIRE

Net force equations summarized by Moeser et al. [14] include magnetic properties like magnetization values and magnetic field strengths, dimension and velocity. In the dimensional terms, coating thickness is additionally considered from the Ying et al. [13]'s equations. They have also considered diffusion force term made by concentration difference between the accumulated area and bulk fluid. Purely drag-limited and diffusion-limited net force equations were summarized as follows:

Purely drag limited:

$$\begin{aligned} & \text{r-direction} \\ 0 = & -\frac{2\mu_0 M_w M_p r_p^3}{9\mu(r_p + r_{coat})r_w^2} \left(\frac{M_w}{2H_o(r_r/r_w)^5} + \frac{\cos 2\theta}{(r_r/r_w)^3} \right) - \frac{V_o}{r_w} \frac{\ln\left(\frac{r_r + r_p + r_{coat}}{r_r}\right) - 0.5 \left(1 - \left(\frac{r_r}{r_r + r_p + r_{coat}}\right)^2\right)}{2.002 - \ln\left(\frac{2V_o \rho_f r_r}{\mu}\right)} \cos \theta \end{aligned} \quad (1)$$

$$\begin{aligned} & \theta\text{-direction} \\ 0 = & -\frac{2\mu_0 M_w M_p r_p^3}{9\mu(r_p + r_{coat})r_w^2} \frac{\sin 2\theta}{(r_\theta/r_w)^3} - \frac{V_o}{r_w} \frac{\ln\left(\frac{r_\theta + r_p + r_{coat}}{r_\theta}\right) + 0.5 \left(1 - \left(\frac{r_\theta}{r_\theta + r_p + r_{coat}}\right)^2\right)}{2.002 - \ln\left(\frac{2V_o \rho_f r_\theta}{\mu}\right)} \sin \theta \end{aligned} \quad (2)$$

Purely diffusion limited:

$$\frac{k_B T}{6\pi\mu(r_p + r_{coat})r_w^2} \frac{1}{N} \frac{dN}{d(r_{diff}/r_w)} = -\frac{2\mu_0 M_w M_p r_p^3}{9\mu(r_p + r_{coat})r_w^2} \left(\frac{M_w}{2H_o(r_{diff}/r_w)^5} + \frac{\cos 2\theta}{(r_{diff}/r_w)^3} \right) \quad (3)$$

It can be summarized as follows:

$$0 = \frac{1}{k_B T / (6\pi\mu(r_p + r_{coat})r_w^2)} \frac{2\mu_0 M_w M_p r_p^3}{9\mu(r_p + r_{coat})r_w^2} \left(\frac{M_w}{8H_o(r_{diff}/r_w)^4} + \frac{\cos 2\theta}{2(r_{diff}/r_w)^2} \right) - \ln \left(\frac{N_{accumulated}}{N_{NF}} \right) \quad (4)$$

$$\text{Where, } N_{accumulated} = \frac{1}{(2(r_p + r_{coat}))^3}$$

Ying et al. [13] included a van der Waals force term, and it can be changed into as follow if the coating thickness is additionally included as done by the Moeser et al. [14]:

$$F_{VDW} = - \frac{2A}{3(r_p + r_{coat}) \left(\frac{r - r_w + (r_p + r_{coat})}{(r_p + r_{coat})} \right)^2 \left(\frac{r - r_w - (r_p + r_{coat})}{(r_p + r_{coat})} \right)^2} r \quad (5)$$

A Hamaker constant, A, value used in the above van der Waals equation has been acquired from Zhang et al. [18]'s research where several combinations of materials have been considered.

Fletcher [19] considered a double layer effect by replacing bulk temperature with sum of the bulk temperature and double layer temperature. Since the equation form is similar, the effective temperature can be represented by sum between two. In the double layer temperature, a potential information is included to account for the interaction between the particles. The effective temperature is represented as follow:

$$T^* = T + T_{DL} \text{ where, } T_{DL} = \frac{4\pi \varepsilon_o \varepsilon_r \psi^2 (r_p + r_{coat})}{3 k_B} \quad (6)$$

3.1. Net Force Equations in This Study

Based on the aforementioned terms, net forces of purely drag-limited and diffusion-limited cases could be summarized as follows:

Purely drag limited:

$$\begin{aligned} & \text{r-direction} \\ 0 = & - \frac{2\mu_0 M_w M_p r_p^3}{9\mu(r_p + r_{coat})r_w^2} \left(\frac{M_w}{2H_o(r_r/r_w)^5} + \frac{\cos 2\theta}{(r_r/r_w)^3} \right) - \frac{V_o}{r_w} \frac{\ln \left(\frac{r_r + r_p + r_{coat}}{r_r} \right) - 0.5 \left(1 - \left(\frac{r_r}{r_r + r_p + r_{coat}} \right)^2 \right)}{2.002 - \ln \left(\frac{2V_o \rho_f r_r}{\mu} \right)} \cos(\theta - \gamma) \\ & - \frac{1}{6\pi\mu r_w (r_p + r_{coat})} \frac{2A}{3(r_p + r_{coat}) \left(\frac{r - r_w + (r_p + r_{coat})}{(r_p + r_{coat})} \right)^2 \left(\frac{r - r_w - (r_p + r_{coat})}{(r_p + r_{coat})} \right)^2} \end{aligned} \quad (7)$$

$$\begin{aligned} & \text{\theta-direction} \\ 0 = & - \frac{2\mu_0 M_w M_p r_p^3}{9\mu(r_p + r_{coat})r_w^2} \frac{\sin 2\theta}{(r_\theta/r_w)^3} - \frac{V_o}{r_w} \frac{\ln \left(\frac{r_\theta + r_p + r_{coat}}{r_\theta} \right) + 0.5 \left(1 - \left(\frac{r_\theta}{r_\theta + r_p + r_{coat}} \right)^2 \right)}{2.002 - \ln \left(\frac{2V_o \rho_f r_\theta}{\mu} \right)} \sin(\theta - \gamma) \end{aligned} \quad (8)$$

Purely diffusion limited:

$$\frac{k_B T^*}{6\pi\mu(r_p + r_{coat})r_w^2} \frac{1}{N} \frac{dN}{d(r_{diff}/r_w)} = - \frac{2\mu_0 M_w M_p r_p^3}{9\mu(r_p + r_{coat})r_w^2} \left(\frac{M_w}{2H_o(r_{diff}/r_w)^5} + \frac{\cos 2\theta}{(r_{diff}/r_w)^3} \right) \quad (9)$$

$$= - \frac{1}{6\pi\mu r_w (r_p + r_{coat})} \frac{2A}{3(r_p + r_{coat}) \left(\frac{r - r_w + (r_p + r_{coat})}{(r_p + r_{coat})} \right)^2 \left(\frac{r - r_w - (r_p + r_{coat})}{(r_p + r_{coat})} \right)^2}$$

It can be summarized as follows:

$$0 = \frac{1}{k_B T^* / (6\pi\mu(r_p + r_{coat})r_w^2)} \left[\int_{\infty}^{r_{diff}} \frac{1}{6\pi\mu r_w (r_p + r_{coat})} \frac{2A}{3(r_p + r_{coat}) \left(\frac{r - r_w + (r_p + r_{coat})}{(r_p + r_{coat})} \right)^2 \left(\frac{r - r_w - (r_p + r_{coat})}{(r_p + r_{coat})} \right)^2} d(r_{diff}/r_w) \right] \quad (10)$$

$$- \ln \left(\frac{N_{accumulated}}{N_{NF}} \right)$$

$$\text{Where, } N_{accumulated} = \frac{1}{(2(r_p + r_{coat}))^3}$$

$$= \frac{1}{6\pi\mu r_w (r_p + r_{coat})} \frac{2A}{3(r_p + r_{coat})} \frac{(r_p + r_{coat})^4}{r_w^4} \frac{r_w^3}{(r_p + r_{coat})^3} \left[0.5 \left\{ \frac{\cos \theta_{r_a}}{(\sin \theta_{r_a})^2} - \ln \left(\frac{1 - \cos \theta_{r_a}}{\sin \theta_{r_a}} \right) \right\} + \ln \left| \frac{\sin(\theta_{r_a}/2)}{\cos(\theta_{r_a}/2)} \right| \right]$$

$$\theta_{r_a} = \sec^{-1} \left(\frac{r_w}{r_p + r_{coat}} \left(\frac{r_{diff}}{r_w} - 1 \right) \right)$$

3.2. Particle Size and Temperature Effects on the Capture

Magnetic core size and coating thickness effects for various temperature conditions have been assessed under an atmospheric pressure condition. Magnetization values of the magnetite and steel wool have been determined from Takayasu et al. [12] and Aviles [20] where an external magnetic field strength is considered. The saturated magnetization values considered in this study were 63 emu/g [14] and 1.35E6 A/m [12], respectively, and direction between the magnetic field and flow was vertical. The other parameters have been fixed for the calculations: Steel wire diameter (50 μm), magnetic field strength (1 T), flow velocity (0.01 m/s), particle concentration (1 ppmV), double layer potential (35 mV). Dots on the figures represent accumulation boundaries around the steel wire; magnetic particles are gathered within the area.

3.2.1. Magnetic core size & silica coating thickness effects

As expected, accumulation around the wire increases with magnetic core size. For whole range of coating thickness considered in the study, the trend was the same as in Fig. 3. In comparison, the amount of the

accumulation decreases with coating thickness (Fig. 4) since volumes occupied by the silica do not possess the magnetic characteristics; rather, it puts some distance.

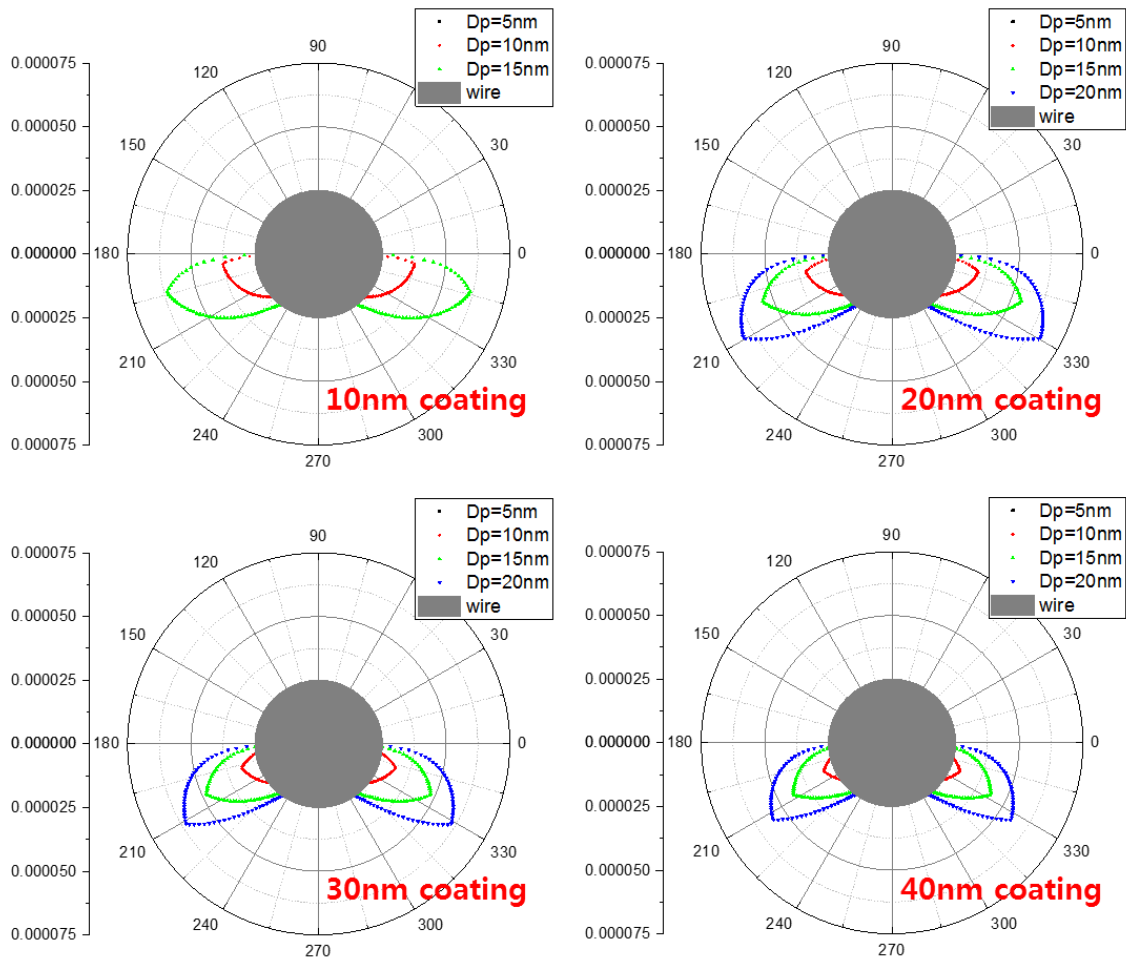


Figure 3. Magnetite Particle Size Effect on the Accumulation Boundary (30 °C).

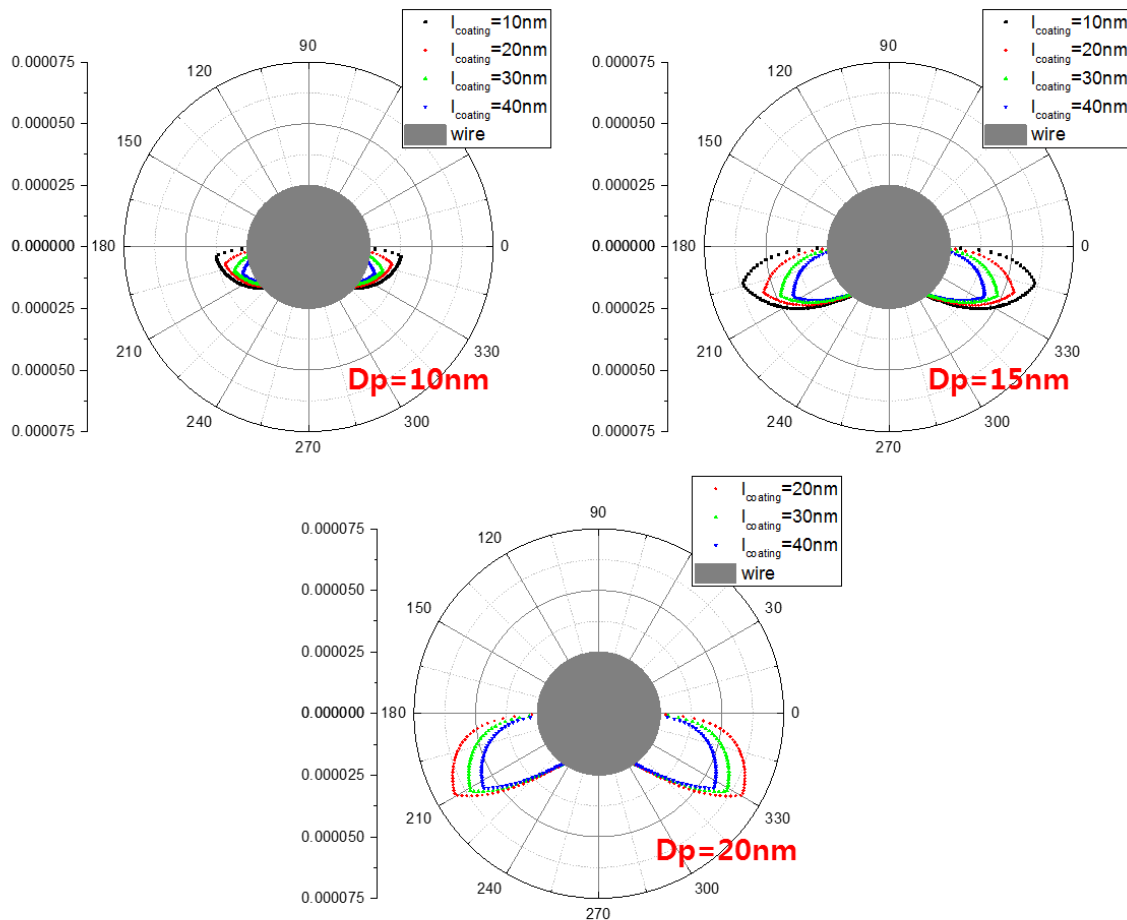


Figure 4. Coating Thickness Effect on the Accumulation Boundary (30 °C).

3.2.2. Temperature effects

Generally, relatively high temperature conditions are expected during the severe accident progression, and temperature effect has been assessed in this section to account for the optimized release moments after the usage.

According to the calculation results, the accumulation decreases with temperature by the diffusion term, made between the accumulated and non-accumulated area. However, the effect was relatively marginal compared with other parametric effects (Fig. 5).

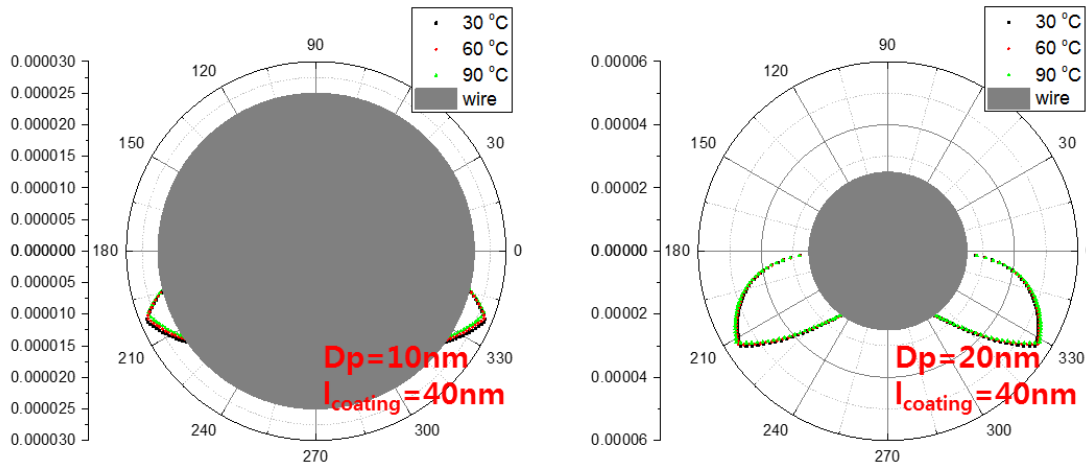


Figure 5. Temperature Effect on the Accumulation Boundary (30, 60, 90 °C).

4. CONCLUSIONS

A system of multi-functional magnetic nanoparticles can be applied to the severe accident mitigations strategies. Porous coating around the magnetic nanoparticle enlarges surface area where the functional groups are attached. Through the system, enhancement of the CHF is expected by deposition, and the removal of target radioactive nuclides from the coolant can be achievable at the same time. With the magnetic characteristics, those particles can be collected; purified coolant can be ejected. Among various parametric effects, particle size & coating thickness effects have been focused in this study with temperature conditions. The accumulation increases with magnetic particle size and decreases with coating thickness according to the calculation results. Also, it decreases with temperature, but the effect was rather marginal compared with other parametric effects. Based on the results, particle size can be designed, at least suggesting a minimum criterion. When considering the real application, initial stage of the system activation should also be considered: injection. In this respect, some patent is enrolled for the purpose [21]. Also, experimental database should be more accumulated and reinforced in the future for the actual applications.

NOMENCLATURE (IF NEEDED)

μ	Viscosity
μ_o	Permeability of free space
M_w	Wire magnetization
M_p	Magnetite magnetization
r_p	Magnetite radius
r_{coat}	Coating thickness
r_w	Wire radius
r_r	Radial force-based accumulation limit line
r_θ	Tangential force-based accumulation limit line
r_{diff}	Diffusion force-based accumulation limit line
H_o	External magnetic field strength
θ	Angle
β	Angle of gravitational force from horizontal axis
γ	Angle of velocity from horizontal axis
V_o	Velocity
ρ_f	Fluid density
ρ_p	Particle density
k_B	Boltzmann constant

T	Temperature
N	Number density
N_{NF}	Nanofluid concentration
$N_{accumulation}$	Number density in accumulation area
g	Gravitational acceleration
ϵ_0	Absolute permittivity
ϵ_r	Relative permittivity of the liquid
ψ	Double layer potential
A	Hamaker constant (10.2E-21 J for silica in water)

ACKNOWLEDGMENTS

This work was supported by the Nuclear Safety Research Program through the Korea Foundation Of Nuclear Safety(KoFONS), granted financial resource from the Nuclear Safety and Security Commission(NSSC), Republic of Korea (No. 1305011), and the National Research Foundation of Korea(NRF) grant funded by the Korea government (No. NRF-2017M2A8A4056643).

REFERENCES

List references here, according to their first use in the paper. Include the following information (as applicable). Do not include these sentences in the full paper:

1. S.J. Kim, T. McKrell, J. Buongiorno, L.-W. Hu, "Subcooled flow boiling heat transfer of dilute alumina, zinc oxide, and diamond nanofluids at atmospheric pressure," *Nucl. Eng. Des.* **240(5)**, pp. 1186-1194 (2010).
2. H.D. Kim, M.H. Kim, "Effect of nanoparticle deposition on capillary wicking that influences the critical heat flux in nanofluids," *Appl. Phys. Lett.* **91(1)**, p. 014104 (2007).
3. S.D. Park, I.C. Bang, "Flow boiling CHF enhancement in an external reactor vessel cooling (ERVC) channel using graphene oxide nanofluid," *Nucl. Eng. Des.* **265**, pp. 310-318 (2013).
4. H.S. Ahn, J.M. Kim, M. Kaviani, M.H. Kim, "Pool boiling experiments in reduced graphene oxide colloids part II - Behavior after the CHF, and boiling hysteresis," *Int. J. Heat Mass Transf.* **78**, pp. 224-231 (2014).
5. J. Yang, F.B. Cheung, J.L. Rempe, K.Y. Suh, S.B. Kim, "Critical heat flux for downward-facing boiling on a coated hemispherical vessel surrounded by an insulation structure," *Nucl. Eng. Technol.* **38**, pp. 139-146 (2006).
6. J.H. Lee, D.H. Kam, Y.H. Jeong, "The effect of nanofluid stability on critical heat flux using magnetite-water nanofluids," *Nucl. Eng. Des.* **292**, pp. 187-192 (2015).
7. T. Lee, J.H. Lee, Y.H. Jeong, "Flow boiling critical heat flux characteristics of magnetic nanofluid at atmospheric pressure and low mass flux conditions," *Int. J. Heat Mass Transf.* **56**, pp. 101-106 (2013).
8. T. Lee, D.H. Kam, J.H. Lee, Y.H. Jeong, "Effects of two-phase flow conditions on flow boiling CHF enhancement of magnetite-water nanofluids," *Int. J. Heat Mass Transf.* **74**, pp. 278-284 (2014).
9. J.H.P. Watson, "Magnetic filtration," *J. Appl. Phys.* **44(9)**, pp.4209-4213 (1973).
10. S. Uchiyama, S. Kondo, M. Takayasu, "PERFORMANCE OF PARALLEL STREAM TYPE MAGNETIC FILTER FOR HGMS," *IEEE Transactions on Magnetics*, **MAG-12(6)**, pp. 895-897 (1976).
11. J.A. Oberteuffer, "High Gradient Magnetic Separation," *IEEE Transactions on Magnetics*, **MAG-9(3)**, pp. 303-306 (1973).
12. M. Takayasu, R. Gerer, F.J. Friedlaender, "MAGNETIC SEPARATION OF SUBMICRON PARTICLES," *IEEE Transactions on Magnetics*, **MAG-19(5)**, pp. 2112-2114 (1983).
13. T.-Y. Ying, S. Yiaccoumi, C. Tsouris, "High-gradient magnetically seeded filtration," *Chem. Eng. Sci.* **55**, pp. 1101-1113 (2000).
14. G.D. Moeser, K.A. Roach, W.H. Green, T.A. Hatton, P.E. Laibinis "High-Gradient Magnetic Separation of Coated Magnetic Nanoparticles," *AIChE* **50(11)**, pp.2835-2848 (2004).
15. F.J. Friedlaender, M. Takayasu, J.B. Rettig, C.P. Kentzer, "Particle Flow and Collection Process in Single Wire HGMS Studies," *IEEE Transactions on Magnetics*, **MAG-14(6)**, pp. 1157-1164 (1978).
16. F. Granados, V. Bertin, S. Bulbulian, M. Solache-Rios, "60Co aqueous speciation and pH effect on the adsorption behavior on inorganic materials," *Appl. Rad. Isotopes*, **64(3)**, pp. 291-297 (2006).

17. X. Feng, G. E. Fryxell, L. -Q. Wang, A. Y. Kim, J. Liu, K. M. Kemner, "Functionalized Monolayers on Ordered Mesoporous Supports," *Sci.*, **276(5314)**, pp. 923-926 (1997).
18. H. Zhang, J.F. Banfield, "Interatomic Coulombic interactions as the driving force for oriented attachment," *CrystEngComm.*, **16**, pp. 1568-1578 (2014).
19. D. Fletcher, "Fine Particle High Gradient Magnetic Entrapment," *IEEE Transactions on Magnetics*, **27(4)**, pp. 3655-3677 (1991).
20. M.O. Aviles, "EXPERIMENTAL AND THEORETICAL STUDIES OF IMPLANT ASSISTED MAGNETIC DRUG TARGETING," Ph.D. Dissertation, University of South Carolina (2008).
21. J.H. Lee, Y.H. Jeong, "Nanofluid injection device for heat removal from nuclear power plants," Registration No. 1014749660000, KAIST, Korea.